Mass yield distributions in the ^{232}Th(n, f) reaction with fast neutrons

H. Naik
Radiochemistry Division, Bhabha Atomic Research Centre, Mumbai-400 085, India

G. N. Kim,* K. Kim, and M. Zaman
Department of Physics, Kyungpook National University, Daegu 41566, Korea

(Received 9 March 2019; published 17 July 2019)

The cumulative yields of 48 fission products in the mass range of 77–153 have been measured for the ^{232}Th(n, f) reaction with the average neutron energies of 7.46, 13.4, and 18.0 MeV using an off-line γ-ray spectrometric technique. Fast neutron beams were generated using the ^{9}Be(p, n) reaction with the proton energies of 25, 35, and 45 MeV from the MC-50 Cyclotron at the Korea Institute of Radiological and Medical Sciences. Post-neutron mass chain yields were obtained from the cumulative fission yields using the charge distribution correction of the medium energy. From the mass yield data, the peak-to-valley ratio, average light mass, and heavy mass, as well as the average neutron numbers were obtained. The fine structure of the mass yield distribution in the ^{232}Th(n, f) reaction is explained by considering the nuclear structure effects such as the even–odd effect and shell closure proximity. The effect of deformed shells closure proximity arising due to the octupole deformation of fragments is discussed. The difference in the mass yield distribution between the ^{232}Th(n, f) and ^{238}U(n, f) reactions at various excitation energies is explained based on the different types of potential energy surfaces between the two fissioning systems. The role of excitation energy on the standard I and standard II asymmetric mode of fission is also discussed. In the ^{232}Th(n, f) reaction with the excitation energies of 11–13 MeV, the onset of symmetric product yields, peak-to-valley ratio, average light mass, and heavy mass, as well as the average neutrons number have been observed, which are explained from the point of second chance fission.

DOI: 10.1103/PhysRevC.100.014606

I. INTRODUCTION

Nuclear fission of actinides induced by neutrons is of importance for reactor applications and investigations into fundamental physics. In particular, the yields of fission products in the neutron-induced fission of actinides are required for decay heat [1] calculations and this information is therefore important in the design of various type of reactor. The fission products yields of actinides related to the ^{238}U-^{239}Pu and ^{232}Th-^{233}U fuel cycles are important for conventional (LWR, BWR), fast reactors [2–5], advanced heavy water reactors (AHWRs) [6], and accelerated driven sub-critical systems [7–9]. Moreover, fission product yields are required for mass and charge distributions studies to examine the effect of nuclear-structure and the dynamics of descent from saddle to scission [10,11]. It is well-known that the mass yield distribution [10,11] in the neutron-induced fission of preactinides and heavy-Z actinides (Es to Lr) are symmetric. In contrast, the mass yield distributions of medium-Z actinides (U to Cf) are asymmetric with a double hump, whereas the light-Z actinides (Ac, Th, Pa) are asymmetric with a triple hump [10,11]. It is also well-established that the mass yield distributions in the low-energy neutron-induced fission of actinides have a fine structure, which has been explained using the standard I and standard II asymmetric mode of fission [12] based on the static scission point model [13] as well as based on deformed shell effect arising from the octupole deformation [14]. In the absence of an even–odd effect, the fine structure of the odd-Z actinides is only due to the effect of shell closure proximity [10,11,13,14]. However, for the even-Z actinides, the nuclear structure effect is due to an even–odd effect [15,16] apart from the shell closure proximity [13,14]. Among all the actinides, low energy neutron-induced fission of ^{229}Th and ^{232}Th have the maximum even–odd effect [15,16] and well-known asymmetric triple-humped mass yield distributions [17,18]. However, with the increase of the excitation energy and Z of the actinides, the effect of nuclear structure decreases and thus, the fine structure of the mass yield distribution is expected to vanish. In addition, with the increase of the excitation energy, the mass yield distribution is also expected to change from an asymmetric to a symmetric type. However, the specific excitation energy at which the nuclear structure vanishes, and the asymmetric mass yield distribution becomes symmetric is still not known. This is most probably due to the unavailability of high energy monoenergetic neutron sources and the increase of the probability of multichance fission with neutron energy.

The mass yield distribution in the ^{232}Th(n, f) reaction has been determined by several experimentalists using reactor neutron [17,18], monoenergetic neutrons from 1.6 to 8 MeV and approximately 14 MeV [19–40] as well as within the average neutron energy ranges of 5.42–13.4 MeV and 18.1 MeV [22,36,41–43]. Monoenergetic neutrons with the energies of approximately 2.45 and 14 MeV as well as within the range

*gnkim@knu.ac.kr

1.6–5.3 MeV are based on the ^{2}H(^{2}H, n), ^{3}H(^{2}H, n), and ^{3}H(p, n) reactions [19–40]. However, the quasimonoenergetic or average neutron energies used in the range of 5.42–13.4 MeV and at 18.1 MeV, are based on the ^{7}Li(d, n) and ^{7}Li(p, n) reactions [22,36,41–43]. According to the literature [19–43], the nuclear structure effect is clearly observed even above the average neutron energies of 12.53 MeV. The fission yields in the ^{232}Th(n, f) reaction with monoenergetic neutron at approximately 13.4–14.9 MeV and at 18.1 MeV are primarily associated with symmetric products, which clearly show a third peak in the mass yield distribution and decreases with an increase of the excitation energy. However, the fine structure of the mass yield distribution was not shown owing to insufficient data for the entire mass chains. The fragment mass yields in the 10–60 MeV quasimonoenergetic neutron-induced fission of ^{232}Th and ^{238}U based on the physical technique are available in the literature [44–46]. The quasimonoenergetic neutron used in Refs. [44–46] are based on the ^{7}Li(p, n) reaction neutron source. In the fragment yield data of the ^{232}Th(n, f) reaction, the peak-to-valley ratio was found to decrease significantly for neutron energy of 10 to 60 MeV. However, in the fission yield data based on the physical technique [44–46], the effect of nuclear structure was not observed owing to fragmented yields. In the neutron energy range of 14.9 to 60 MeV, the experimental data are not available from off-line gamma-ray spectrometric technique to examine the fine structure in the mass yield distribution of the ^{232}Th(n, f) reaction. Even for the fission yield data within the neutron energies of 13.4–14.9 MeV, the fine structure in the mass yield distribution is not shown owing to insufficient data for the entire mass chains.

In view of the above-mentioned facts, in the present work, the cumulative yields of various fission products in the ^{232}Th(n, f) reaction with average neutron energies of 7.46, 13.4, and 18.0 MeV was investigated using an off-line γ-ray spectrometric technique. The average neutron energies were obtained from the ^{9}Be(p, n) reaction using the proton energies of 25, 35, and 45 MeV. From the cumulative yields of the fission products, their mass chain yields were obtained using the charge distribution correction [47,48]. The mass yield distribution parameters such as the peak-to-valley (P/V) ratio, average light mass ($\langle A_L \rangle$), heavy mass ($\langle A_H \rangle$), and the average neutron number ($\langle \upsilon \rangle$) were also obtained. The presented data for the three average neutron energies and the literature data [19–43] at other neutron energies from the ^{232}Th(n, f) reaction are compared with similar available data in EXFOR [49] for the ^{238}U(n, f) reaction [50–57] to examine the role of the excitation energy on the nuclear structure effect and the mass yield distribution parameters.

II. EXPERIMENTAL PROCEDURE

The present experiment was performed using the MC-50 Cyclotron at the Korean Institute of Radiological and Medical Sciences (KIRAMS), Korea. Three ^{232}Th metal foils with >99.99% purity, 0.025-mm thickness, and 192.3, 270.0, and 285.6 mg weight were separately wrapped with 0.025-mm-thick Al foils with a purity of more than 99.99%. The aluminum wrapper foil acts as a catcher for the fission products that recoil out from the surface of the thorium metal foil during the irradiation process. Fast neutrons were produced from the ^{9}Be(p, n) reaction by impinging proton beam with energies of 25, 35, and 35 MeV from the cyclotron onto a 5-mm-thick beryllium target. The 25 MeV proton beam was completely stopped in the 5-mm-thick Be foil. However, the 35 and 45 MeV proton beams partial passed through the Be-target. Therefore, 0.45- and 1.05-mm-thick tantalum foils were placed behind the Be-target to completely stop the 35 and 45 MeV proton beam, respectively. The neutron spectra from the ^{9}Be(p, n) reaction were generated using a computer code MCNPX 2.6.0 [58] and are presented in Fig. 1.

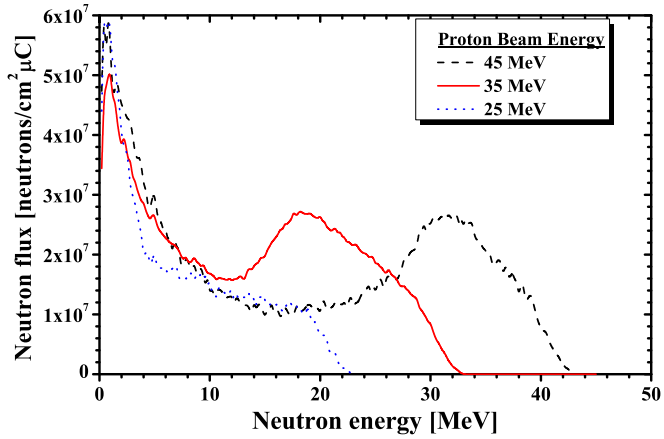

FIG. 1. Neutron spectra calculated using MCNP code [58] for the ^{9}Be(p, n) reaction for proton with energies of 25, 35, and 45 MeV bombarding a 5-mm-thick Be foil.

The target sample assemblies were fixed individually on a stand and positioned at an appropriate height in the air at a distance of 2.8 cm behind the Be-target. The sample assemblies were then irradiated for 0.5, 1, and 1 h, respectively, with neutron beams generated from the bombardment of 45, 35, and 25 MeV proton beams incident on the Be target. The diameter of the proton beam collimator was 10 mm. The proton beam current during irradiation for all three experiments was approximately 200 nA. The irradiated ^{232}Th samples along with the Al wrapper were removed from the irradiated assembly after cooling times of 1.186, 0.605, and 0.726 h, respectively. They were mounted on separate Perspex (acrylic glass, 1.5-mm-thick) plates. The γ-ray counting of the fission products from the Al-wrapped ^{232}Th-irradiated samples was performed using an energy and efficiency-calibrated HPGe detector coupled to a PC-based 4K-channel analyzer. The resolution of the detector was 1.8 keV full-width at half-maximum (FWHM) at 1332.5 keV γ-ray photopeak of ^{60}Co. A standard source ^{152}Eu was used for the energy and the efficiency calibration. The detector efficiency was 20% for the 1332.5 keV γ-ray photopeak relative to a 7.6 cm diameter × 7.6 cm length NaI(Tl) detector. During the γ-ray counting, the dead time of the HPGe detector system was always maintained below 5% by placing the sample at an appropriate distance to avoid pile up and coincidence-summing effects. This was examined by determining the efficiency of the detector system for the same geometry using mono or di-energetic

γ-ray sources such as ^{241}Am (59.54 keV), ^{57}Co (122.1 keV), ^{137}Cs (661.7 keV), ^{54}Mn (834.8 keV), and ^{60}Co (1173.2 and 1332.5 keV). Therefore, a ^{152}Eu source with a γ-ray energy range of 121.8–1408.0 keV was used to avoid the complexity of using many standards with one or a few γ-lines each. The γ-ray counting of the samples was performed in live time mode on several occasions with an increase of counting time depending on the half-life of the radionuclides of interest.

III. DATA ANALYSIS AND RESULTS

A. Calculation of average neutron energy and excitation energy

The neutron flux in the experiments for three different energies was produced from the ^{9}Be(p, n) reaction. As previously indicated, the neutron spectra from the ^{9}Be(p, n) reaction were generated using computer code MCNPX 2.6.0 [58]. From the neutron spectra, the average neutron energy within the range of threshold values to the maximum neutron energy ($\langle E_n \rangle$) was calculated using the following equation:

$$\langle E_n \rangle = \int_{E_{\rm th}}^{E_{\rm max}} E_n\, \varphi(E_n)\, dE_n \Big/ \int_{E_{\rm th}}^{E_{\rm max}} \varphi(E_n)\, dE_n, \qquad (1)$$

where $\varphi(E_n)$ is the neutron flux as a function of neutron energy as shown in Fig. 1. The flux-weighted average neutron energies ($\langle E_n \rangle$) based on the ^{9}Be(p, n) reaction for the three proton energies of 25, 35, and 45 MeV are 7.46, 13.4, and 18.0 MeV, respectively.

From the average neutron energy ($\langle E_n \rangle$), the average excitation energy ($\langle E^* \rangle$) of the compound nucleus ^{233}Th* in the ^{232}Th(n, f) reaction was calculated using the following relation:

$$\langle E^* \rangle = (\Delta_{^{232}\rm Th} + \Delta_n - \Delta_{^{232}\rm Th}) + \langle E_n \rangle, \qquad (2)$$

where Δ is the mass excess taken from the nuclear wallet cards [59]. For the compound nucleus ^{233}Th*, the average excitation energies corresponding to the average neutron energies of 7.46, 13.4, and 18.0 MeV are 12.25, 18.19, and 22.79 MeV, respectively.

B. Calculation of fission product yields

From the total photopeak activities, the number of detected ($N_{\rm obs}$) γ-rays for the fission products of interest was obtained by subtracting the linear Compton background. From $N_{\rm obs}$ of an individual fission product, the cumulative yields (Y_R) relative to ^{92}Sr were calculated using the decay equation [42,43],

$$Y_R = \frac{N_{\rm obs}({\rm CL}/{\rm LT})\lambda}{n\,\sigma_f\,\varphi\,I_\gamma\,\varepsilon\,(1-e^{-\lambda t})e^{-\lambda T}(1-e^{-\lambda\,{\rm CL}})}, \qquad (3)$$

where n is the number of target atoms, φ is the neutron flux, and σ_f is the flux-weighted average fission cross-section of the ^{232}Th(n, f) reaction at the average neutron energies of 7.46, 13.4, and 18.0 MeV. I_γ is the γ-ray intensity or γ-ray emission probability, ε is the detection efficiency of the γ-rays in the detector system, and λ is the decay constant ($\lambda = \ln 2/T_{1/2}$) of the fission-product of interest. t and T are the irradiation and cooling times, whereas CL and LT are the real time and the live time of counting, respectively.

To calculate the fission yield, it is necessary to calculate separately the individual n,σ_f and φ terms. However, in the present work, the combined $n\sigma_f\varphi$ term was obtained from the photopeak activity of the 1383.9 keV γ-line of ^{92}Sr by assuming its cumulative yield (Y_R) to be 1.0. Using the $n\sigma_f\varphi$ term in Eq. (3), the relative cumulative yields (Y_R) of the other fission products were then obtained from the photopeak activities of the γ-lines of the corresponding fission products. Nuclear spectroscopic data, such as the γ-ray energies, the half-lives ($T_{1/2}$), and the γ-ray intensity (I_γ) of the fission products used in Eq. (3) were taken from the literature [60,61] and are given in Table I.

From the Y_R values of the fission products, their relative mass-chain yields (Y_{RA}) were calculated using the Wahl's prescription [47] followed by a charge distribution correction based on the work of Umezawa *et al.* [48] for medium energy fission. According to Wahl's result [47], the fractional cumulative yield ($Y_{\rm FCY}$) of a fission product in an isobaric mass chain is given as follows:

$$Y_{\rm FCY} = \frac{{\rm EOF}^{a(Z)}}{\sqrt{2\pi\,\sigma_Z^2}} \int_{-\infty}^{Z+0.5} \exp\left[-(Z-Z_P)^2/2\sigma_Z^2\right] dZ, \qquad (4a)$$

$$Y_{RA} = Y_R/Y_{\rm FCY}, \qquad (4b)$$

where Z_P is the most probable charge and σ_z is the width parameter of an isobaric-yield distribution. EOF$^{a(Z)}$ is the even–odd effect with $a(Z) = +1$ for even-Z nuclides and -1 for odd-Z nuclides. It can be seen from Eqs. (4a) and (4b) that for the calculation of the $Y_{\rm FCY}$ value and the relative mass-chain yield (Y_{RA}) of fission product, it is necessary to know Z_P, σ_z, and EOF$^{a(Z)}$. It has been established that the EOF$^{a(Z)}$ values in medium energy fission are negligible [10,11]. In the ^{232}Th(n, f) reaction with an average neutron energy of 1.9 MeV, an average σ_z value of 0.52±0.08 was experimentally obtained earlier [16], Similarly, Umezawa *et al.* [48] have shown that the average σ_z value for medium energy protons and α-induced fission of ^{232}Th and ^{238}U is 0.70 ± 0.06. Thus, in the present work, we used the average σ_z value of 0.6, 0.62, and 0.65 at the average neutron energies of 7.46, 13.4, and 18.0 MeV, respectively. Then the Z_P values of the individual mass chain (A) in the ^{232}Th(n, f) reaction at average neutron energies of 7.46, 13.4, and 18.0 MeV was calculated based the prescription of Umezawa *et al.* [48] as

$$Z_P = \eta\, Z_F \pm \Delta Z_P, \quad \eta\, Z_F = Z_{\rm UCD} = (Z_F/A_F)(A + \upsilon_{\rm post}), \qquad (5a)$$

$$\eta = (A + \upsilon_{\rm post})/(A_C - \upsilon_{\rm pre}), \quad A_F = A_C - \upsilon_{\rm pre}, \qquad (5b)$$

where Z_C and A_C are the charge and mass of the compound nucleus (^{233}Th*). $Z_{\rm F}$ and $A_{\rm F}$ are the charge and mass of the fissioning system. $Z_{\rm UCD}$ is the most probable charge based on the unchanged charge-density distribution as suggested by Sugarman and Turkevich [62]. A is the mass of the fission product and $\Delta Z_{\rm P}(=Z_{\rm P} - Z_{\rm UCD})$ is the charge-polarization parameter. The + and − signs for the ΔZ_P value are applicable to light and heavy fragments, respectively. $\upsilon_{\rm pre}$ and $\upsilon_{\rm post}$ are the

TABLE I. Nuclear spectroscopic data and yields of the fission products (%) for the ^{232}Th(n, f) reaction with average neutron energies of 7.46, 13.4, and 18.0 MeV.

Nuclide	Half-life	γ-energy (keV)	γ-abundance (%)[b]	Average neutron energy (MeV)					
				7.46		13.4		18.0	
				Y_C (%)	Y_A (%)	Y_C (%)	Y_A (%)	Y_C (%)	Y_A (%)
^{77}Ge	11.3 h	264.6	53.3 ± 0.5	0.136 ± 0.019	0.136 ± 0.019	0.127 ± 0.025	0.127 ± 0.025	0.179 ± 0.008	0.179 ± 0.008
		416.3	22.7 ± 1.1	0.141 ± 0.009	0.141 ± 0.009	0.166 ± 0.017	0.166 ± 0.017	0.167 ± 0.007	0.167 ± 0.007
^{78}Ge	88.0 min	277.3	96.0 ± 0.1	0.314 ± 0.022	0.314 ± 0.022	0.330 ± 0.050	0.330 ± 0.050	0.348 ± 0.064	0.348 ± 0.064
^{84}Br	31.76 min	1015.9	6.2 ± 0.8	4.880 ± 0.166	4.882 ± 0.166	4.198 ± 0.384	4.198 ± 0.384	3.192 ± 0.256	3.192 ± 0.256
		1897.6	14.6 ± 2.0	4.978 ± 0.213	4.979 ± 0.213	4.118 ± 0.212	4.118 ± 0.212	3.405 ± 0.217	3.405 ± 0.217
^{85m}Kr	4.48 h	151.2	75.2 ± 0.5	5.121 ± 0.383	5.128 ± 0.383	4.729 ± 0.323	4.733 ± 0.323	4.495 ± 0.512	4.501 ± 0.512
		304.9	14.0 ± 0.3	5.644 ± 0.301	5.652 ± 0.301	4.570 ± 0.380	4.574 ± 0.380	4.480 ± 0.528	4.486 ± 0.529
^{87}Kr	76.3 min	402.6	50.0 ± 3.0	4.795 ± 0.285	4.795 ± 0.285	4.279 ± 0.313	4.279 ± 0.313	4.132 ± 0.216	4.133 ± 0.216
^{88}Kr	2.83 h	196.3	26.0 ± 1.2	4.387 ± 0.227	4.392 ± 0.227	4.000 ± 0.101	4.008 ± 0.101	4.038 ± 0.148	4.043 ± 0.148
^{89}Rb	15.32 min	1031.9	63.0 ± 3.0	6.656 ± 0.328	6.656 ± 0.328	5.937 ± 0.516	5.937 ± 0.516	5.858 ± 0.315	5.858 ± 0.315
		1248.1	46.0 ± 3.0	6.478 ± 0.484	6.478 ± 0.484	6.080 ± 0.367	6.080 ± 0.367	5.835 ± 0.306	5.835 ± 0.306
^{91}Sr	9.65 h	749.8	23.6 ± 0.7	5.829 ± 0.296	5.835 ± 0.296	5.068 ± 0.252	5.071 ± 0.252	4.884 ± 0.179	4.884 ± 0.179
		1024.3	33.5 ± 1.1	5787 ± 0.237	5.793 ± 0.237	5.075 ± 0.272	5.079 ± 0.272	4.834 ± 0.226	4.834 ± 0.226
^{92}Sr	2.66 h	1383.9	90.0 ± 6.0	5.130 ± 0.513	5.130 ± 0.513	4.587 ± 0.276	4.587 ± 0.276	4.449 ± 0.345	4.449 ± 0.345
^{93}Y	10.18 h	266.9	7.4 ± 1.1	4.409 ± 0.187	4.412 ± 0.187	4.265 ± 0.552	4.272 ± 0.553	3.972 ± 0.494	3.974 ± 0.494
^{94}Y	18.7 min	918.7	56.0 ± 3.0	4.686 ± 0.217	4.688 ± 0.217	4.483 ± 0.244	4.483 ± 0.244	4.196 ± 0.070	4.196 ± 0.070
^{95}Zr	64.032 days	724.2	44.27 ± 0.22	5.995 ± 0.235	5.995 ± 0.235	5.615 ± 0.403	5.616 ± 0.403	5.403 ± 0.407	5.406 ± 0.407
^{97}Zr	16.749 h	743.4	93.09 ± 0.16	5.019 ± 0.352	5.019 ± 0.352	4.519 ± 0.224	4.519 ± 0.224	4.204 ± 0.509	4.204 ± 0.509
^{99}Mo	65.976 h	140.5	89.43 ± 2.3	2.956 ± 0.342	2.958 ± 0.343	2.762 ± 0.260	2.762 ± 0.260	2.698 ± 0.132	2.698 ± 0.132
		739.5	12.13 ± 1.2	3.058 ± 0.379	3.060 ± 0.380	2.830 ± 0.184	2.830 ± 0.184	2.582 ± 0.140	2.582 ± 0.140
^{101}Mo	14.61 min	590.1	19.2 ± 0.9	1.554 ± 0.074	1.556 ± 0.074	1.701 ± 0.236	1.704 ± 0.237	1.727 ± 0.283	1.728 ± 0.284
^{103}Ru	39.247 days	497.1	91.0 ± 1.2	0.698 ± 0.167	0.698 ± 0.167	1.024 ± 0.092	1.025 ± 0.092	1.086 ± 0.066	1.087 ± 0.066
^{104}Tc	18.3 min	358.0	89.0 ± 3.0	0.444 ± 0.088	0.445 ± 0.088	0.885 ± 0.132	0.885 ± 0.132	1.009 ± 0.151	1.009 ± 0.151
^{105}Ru	4.44 h	724.2	47.3 ± 0.5	0.195 ± 0.048	0.195 ± 0.048	0.812 ± 0.168	0.812 ± 0.168	0.933 ± 0.058	0.934 ± 0.058
^{105}Rh	35.36 h	318.9	19.1 ± 0.6	0.205 ± 0.031	0.205 ± 0.031	0.817 ± 0.088	0.817 ± 0.088	0.969 ± 0.170	0.969 ± 0.170
^{107}Rh	21.7 min	302.8	66.0 ± 6.0	0.217 ± 0.044	0.217 ± 0.044	0.925 ± 0.168	0.925 ± 0.168	1.009 ± 0.089	1.009 ± 0.089
^{112}Ag	3.13 h	617.5	43.0 ± 5.0	0.239 ± 0.024	0.239 ± 0.024	0.969 ± 0.172	0.969 ± 0.172	1.363 ± 0.330	1.363 ± 0.330
^{113}Ag	5.37 h	298.3	10.1	0.243 ± 0.019	0.243 ± 0.019	0.940 ± 0.071	0.940 ± 0.071	1.507 ± 0.315	1.507 ± 0.315
^{115g}Cd	53.46 h	336.2	45.9 ± 1.0	0.205 ± 0.015		0.881 ± 0.156		1.176 ± 0.163	
		527.9	27.45 ± 1.8	0.212 ± 0.046		0.889 ± 0.120		1.335 ± 0.089	
$^{115(m+g)}$Cd				0.243 ± 0.048[a]	0.243 ± 0.048	1.033 ± 0.156[a]	1.033 ± 0.156	1.467 ± 0.163[a]	1.467 ± 0.163
^{117m}Cd	3.36 h	1066.0	23.1 ± 0.7	0.071 ± 0.011		0.376 ± 0.020		0.551 ± 0.104	
		1997.3	26.2 ± 0.5	0.074 ± 0.016		0.349 ± 0.028		0.566 ± 0.112	
^{117g}Cd	2.49 h	273.3	27.9 ± 0.7	0.175 ± 0.013		0.642 ± 0.145		0.892 ± 0.149	
$^{117(m+g)}$Cd				0.248 ± 0.020	0.248 ± 0.020	1.005 ± 0.148	1.005 ± 0.148	1.451 ± 0.151	1.452 ± 0.151
^{127}Sb	3.85 d	685.7	36.8 ± 2.0	0.479 ± 0.103	0.480 ± 0.103	0.910 ± 0.157	0.911 ± 0.157	1.077 ± 0.066	1.079 ± 0.066
^{128}Sn	59.07 min	482.3	59.0 ± 7.0	0.648 ± 0.060	0.714 ± 0.067	1.005 ± 0.060	1.212 ± 0.072	0.943 ± 0.062	1.256 ± 0.083
^{129}Sb	4.366 h	812.97	48.2 ± 0.8	0.932 ± 0.103	0.940 ± 0.104	1.453 ± 0.136	1.485 ± 0.138	1.603 ± 0.142	1.677 ± 0.148
^{131}Sb	23.03 min	943.4	47.1 ± 2.4	1.694 ± 0.143	2.001 ± 0.169	1.841 ± 0.176	2.472 ± 0.235	1.766 ± 0.109	2.722 ± 0.168
^{131}I	8.0252 days	364.5	81.5 ± 0.8	2.273 ± 0.106	2.273 ± 0.106	2.524 ± 0.273	2.524 ± 0.273	2.744 ± 0.124	2.745 ± 0.124
^{132}Te	3.204 days	228.2	88.0 ± 3.0	3.479 ± 0.393	3.537 ± 0.399	3.563 ± 0.180	3.717 ± 0.188	3.614 ± 0.198	3.906 ± 0.214
^{133}I	20.83 h	529.9	87.0 ± 2.3	5.547 ± 0.615	5.551 ± 0.616	5.444 ± 0.488	5.454 ± 0.489	5.435 ± 0.365	5.471 ± 0.367
^{134}Te	41.8 min	566.0	18.6 ± 1.0	4.663 ± 0.097	6.061 ± 0126	3.939 ± 0.180	6.128 ± 0.280	3.245 ± 0.109	5.996 ± 0.201
		767.2	29.5 ± 1.4	5.209 ± 0.166	6.771 ± 0.216	3.979 ± 0.212	6.190 ± 0.330	3.265 ± 0.248	6.032 ± 0.459
^{134}I	52.5 min	847.0	96.0 ± 3.0	6.619 ± 0.436	6.646 ± 0.438	6.035 ± 0.306	6.134 ± 0.311	5.864 ± 0.449	6.079 ± 0.476
		884.1	65.1 ± 2.3	6.443 ± 0.360	6.468 ± 0.361	6.266 ± 0.443	6.369 ± 0.451	5.945 ± 0.400	6.162 ± 0.414
^{135}I	6.58 h	1131.5	22.6 ± 0.7	5.167 ± 0.113	5.340 ± 0.116	4.522 ± 0.205	4.568 ± 0.207	4.523 ± 0.425	5.075 ± 0.476
		1260.4	28.7 ± 0.9	5.566 ± 0.117	5.753 ± 0.121	4.365 ± 0.185	4.409 ± 0.187	4.542 ± 0.543	5.163 ± 0.618
^{138g}Cs	33.41 min	1435.8	76.3 ± 0.5	6.726 ± 0.291	6.736 ± 0.292	6.749 ± 0.244	6.758 ± 0.245	6.273 ± 0.322	6.304 ± 0.324
		1009.8	29.8 ± 0.6	7.115 ± 0.346	7.125 ± 0.347	6.965 ± 0.344	6.975 ± 0.345	6.588 ± 0.256	6.620 ± 0.257
		462.8	30.8 ± 0.7	6.502 ± 0.516	6.511 ± 0.517	6.851 ± 0.235	6.860 ± 0.236	6.265 ± 0.271	6.295 ± 0.274
^{139}Ba	83.06 min	165.9	23.7 ± 0.4	7.540 ± 0.430	7.540 ± 0.430	6.205 ± 0.312	6.205 ± 0.312	5.214 ± 0.543	5.217 ± 0.544
^{140}Ba	12.7527 days	537.3	24.39 ± 0.22	7.402 ± 0.356	7.414 ± 0.357	5.444 ± 0.320	5.451 ± 0.320	4.833 ± 0.295	4.843 ± 0.296

TABLE I. *(Continued.)*

Nuclide	Half-life	γ-energy (keV)	γ-abundance (%)[b]	Average neutron energy (MeV)					
				7.46		13.4		18.0	
				Y_C (%)	Y_A (%)	Y_C (%)	Y_A (%)	Y_C (%)	Y_A (%)
^{141}Ba	18.27 min	190.3	45.5 ± 2.0	5.051 ± 0.257	5.053 ± 0.257	4.435 ± 0.129	4.449 ± 0.129	4.262 ± 0.420	4.265 ± 0.422
^{141}Ce	32.511 d	145.4	48.4 ± 0.3	5.943 ± 0.590	5.943 ± 0.590	4.464 ± 0.279	4.464 ± 0.279	4.252 ± 0.205	4.252 ± 0.205
^{142}La	91.1 min	641.3	47.4 ± 0.5	4.954 ± 0.211	4.954 ± 0.211	4.572 ± 0.242	4.577 ± 0.242	4.485 ± 0.243	4.490 ± 0.243
^{143}Ce	33.039 h	293.3	42.8 ± 0.4	5.954 ± 0.379	5.963 ± 0.380	4.960 ± 0.228	4.960 ± 0.228	4.514 ± 0.422	4.514 ± 0.422
^{146}Pr	24.15 min	453.9	46.0 ± 3.0	4.339 ± 0.145	4.341 ± 0.145	3.697 ± 0.213	3.697 ± 0.213	3.491 ± 0.349	3.491 ± 0.349
		1524.8	15.0 ± 1.0	4.104 ± 0.317	4.105 ± 0.317	3.502 ± 0.279	3.502 ± 0.279	3.064 ± 0.093	3.064 ± 0.093
^{147}Nd	10.98 days	531.0	13.4 ± 0.3	2.275 ± 0.384	2.275 ± 0.384	1.858 ± 0.149	1.858 ± 0.149	1.886 ± 0.254	1.888 ± 0.254
^{149}Nd	1.728 h	211.3	25.9 ± 1.4	1.189 ± 0.069	1.189 ± 0.069	1.077 ± 0.108	1.077 ± 0.108	1.044 ± 0.151	1.045 ± 0.151
		270.2	10.7 ± 0.5	1.249 ± 0.125	1.249 ± 0.125	1.053 ± 0.164	1.053 ± 0.164	1.064 ± 0.206	1.064 ± 0.206
^{149}Pm	53.08 h	285.95	3.1 ± 0.2	1.328 ± 0.356	1.328 ± 0.356	1.133 ± 0.124	1.133 ± 0.124	1.137 ± 0.241	1.137 ± 0.241
^{151}Pm	28.4 h	340.1	22.5 ± 0.9	0.588 ± 0.120	0.588 ± 0.120	0.669 ± 0.028	0.669 ± 0.028	0.687 ± 0.070	0.687 ± 0.070
^{153}Sm	46.284 h	103.2	29.25 ± 0.25	0.209 ± 0.008	0.209 ± 0.008	0.212 ± 0.034	0.212 ± 0.034	0.222 ± 0.029	0.222 ± 0.029

Y_c–Cumulative yields, Y_A–Mass yields, ^{92}Sr–Fission rate monitor.
[a]The yields of $^{115(m+g)}$Cd are based on the ratio of ^{115g}Cd/^{115m}Cd = 6 as done in Ref. [43].
[b]NuDat 2.6, National Nuclear Data Center, Brookhaven National Laboratory, updated 2011, available at http://www.nndc.bnl.gov/.

pre- and post-fission neutrons at scission, that were calculated from the average excitation energy ($\langle E^* \rangle$) of the compound nucleus using the following relations [48].

$$\upsilon_{\text{pre}} = \frac{\langle E^* \rangle}{7.5 \pm 0.5} + \frac{Z_C}{2A_C} - (19.0 \pm 0.5), \tag{6a}$$

$$\upsilon_{\text{post}} = \begin{cases} 1.0 & \text{for} \quad A > 88 \\ 1.0 + 0.1(A - 88) & \text{for} \quad 78 < A < 88 \\ 0 & \text{for} \quad A < 78 \end{cases}. \tag{6b}$$

As previously indicated, for the average neutron energies of 7.46, 13.4, and 18.0 MeV, the average excitation energy ($\langle E^* \rangle$) of the compound nucleus are 12.25, 18.19, and 22.79 MeV, respectively. The $\langle E^* \rangle$ values were used in Eq. (6a) to calculate the υ_{pre} values at three different neutron energies. For the average neutron energies of 7.46, 13.4, and 18.0 MeV, the υ_{pre} values were found to be 0.015, 0.807, and 1.42, respectively. The υ_{pre} and υ_{post} values obtained from Eqs. (6a) and (6b) were used in Eqs. (5a) and (5b) to calculate the value of Z_{UCD} as a function of mass number for the different fission products. The ΔZ_P value was then calculated from the relation given below [48], except for $|\eta - 0.5| < 0.085$, where the charge polarization tends to vanish:

$$\Delta Z_P = 0.35 \times |\eta - 0.5|. \tag{7a}$$

For the region of η value within the $|\eta - 0.5| < 0.085$, the ΔZ_P is given by the following relations:

$$\Delta Z_P = 0 \quad \text{for} \quad |\eta - 0.5| < 0.04, \tag{7b}$$

$$\Delta Z_P = (20/3)(|\eta - 0.5| - 0.04) \quad \text{for} \quad 0.04 < |\eta - 0.5| < 0.085. \tag{7c}$$

The Z_P value as a function of the mass number and the average width parameter (σ_z) of 0.6–0.65 were used in Eq. (4a) to obtain the Y_{FCY} values for individual fission products. The relative mass-chain yield (Y_{RA}) of the fission products based on their relative cumulative yield (Y_R) were obtained in Eq. (4b) using the Y_{FCY} values of different fission products. The relative mass-chain yields (Y_{RA}) of the fission products obtained were then normalized to a total yield of 200% to calculate the absolute mass chain yields (Y_A). The absolute cumulative yields (Y_C) of the fission products in the 7.46, 13.4, and 18.0 MeV neutron-induced fission of ^{232}Th were then obtained from the mass chain yield data and Y_{FCY} values using Eq. (8), which is the modified from Eq. (4b):

$$Y_C = Y_A \times Y_{\text{FCY}}. \tag{8}$$

The absolute cumulative yields (Y_C) and the mass-chain yields (Y_A) of the fission products in the ^{32}Th(n, f) reaction at the average neutron energies of 7.46, 13.4, and 18.0 MeV along with the nuclear spectroscopic data [60,61] are given in Table I. The uncertainty represented in the measured cumulative yield of the individual fission products shown in Table I is the statistical fluctuation of the mean value from replicate measurements. The overall uncertainty is the contributions from both random and systematic errors. The random error is due to the counting statistics of the observed activity and is estimated to be 2–10%. This error can be determined by accumulating data for an optimum period of time, depending on the half-life of the nuclide of interest. The overall systematic error is approximately 3.8–10.5%, which arises from the uncertainties in the irradiation time (0.5%), detector efficiency calibration (∼3%), half-life of the fission products (∼1%), and γ-ray intensity (2–10%) [60,61]. Thus, for the yields of the fission-products, an upper limit of the uncertainty of 4.3–14.5% was obtained based on 2–10% random error and a 3.8–10.5% systematic error.

IV. DISCUSSION

In the present work, the cumulative yields (Y_C) of 48 fission products and the mass yields (Y_A) of 42 isobaric chains in the ^{232}Th(n, f) reaction induced by average neutron energies of

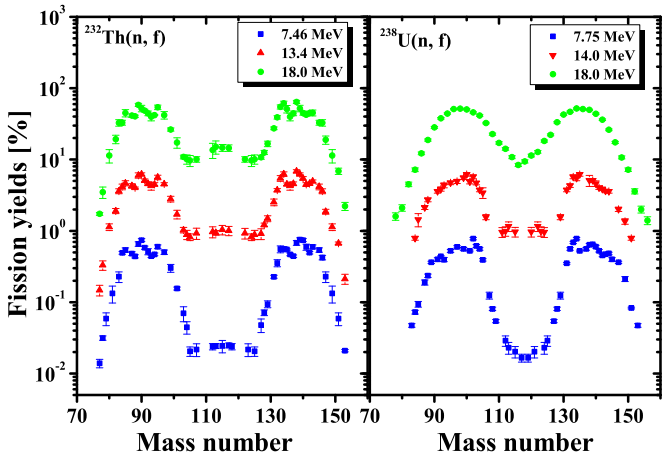

FIG. 2. Mass chain yield distribution in log scale for the ^{232}Th(n, f) reaction with average neutron energies of 7.46, 13.4, and 18.0 MeV as well as for the ^{238}U(n, f) reaction with average neutron energies of 7.75, 14.0, and 18.0 MeV.

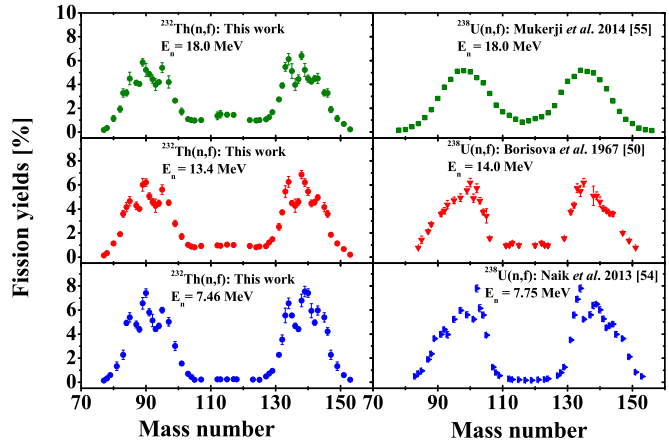

FIG. 3. Mass chain yield distribution in linear scale for the ^{232}Th(n, f) reaction with average neutron energies of 7.46, 13.4, and 18.0 MeV as well as for the ^{238}U(n, f) reaction with average neutron energies of 7.75, 14.0, and 18.0 MeV.

7.46, 13.4, and 18.0 MeV have been measured. The cumulative yields of asymmetric fission products in the ^{232}Th(n, f) reaction for average neutron energies of 13.4 and 18.0 MeV are shown in Table I and are determined for the first time. For symmetric fission products, the cumulative yields for average neutron energies of 13.4 and 18.1 MeV are the redermined values and are in close agreement with the literature data [22] at 13.4 and 18.1 MeV. Similarly, the cumulative yields for both the asymmetric and symmetric products based on the present work for an average neutron energy of 7.46 MeV are also in close agreement with the literature data [36] at 7.6 MeV. The literature data [22,36] are based on quasi monoenergetic neutrons from ^{7}Li(d, n) and ^{7}Li(p, n) reactions, whereas the present data are for the flux-weighted average neutron energies based on ^{9}Be(p, n) reaction. It can be seen from Fig. 1 that the neutron spectrum for the ^{9}Be(p, n) reaction with the proton energy of 25 MeV is broad one with large tail. In spite of very broad neutron spectrum with large tail for the ^{9}Be(p, n) reaction, the fission product yields in the ^{232}Th(n, f) reaction at an average neutron energy of 7.46 MeV are found to be in agreement with the data obtained at 7.6 MeV neutron based on the ^{7}Li(p, n) reaction [36]. This may be due to the use of flux-weighted average energy for the ^{9}Be(p, n) reaction neutron.

The mass chain yield data in the ^{232}Th(n, f) reaction based on the present work at the average neutron energies of 7.46, 13.4, and 18.0 MeV are plotted as a function of their mass number in a log scale in Fig. 2 and in a linear scale in Fig. 3. In the same figures, the fission products yields in the ^{238}U(n, f) reaction at the neutron energies of 7.7 and 14.0 MeV from the literature [51,54], of comparable excitation energies, are also plotted for comparison. In the ^{238}U(n, f) reaction, the yield of highly asymmetric and symmetric products based on the off-line method is available at the neutron energies of 17.7–18.1 MeV [22,50]. For asymmetric products, fission yield data based on the off-line method for neutron energy of approximately 18 MeV are not available in the literature. However, the fission yields of even–even asymmetric and symmetric products at a neutron energy of approximately 18 MeV based on the on-line time-of-flight (TOF) method are available in the literature [57] and are plotted in Figs. 2 and 3 for comparison. It can be seen from Fig. 2 that within the neutron energy range of 7.46–18 MeV, the mass yield distribution in the ^{232}Th(n, f) reaction is triple-humped unlike in the case of the ^{238}U(n, f) reaction where it is double-humped. Figure 2 also shows that in both the ^{232}Th(n, f) and ^{238}U(n, f) reactions, the yields of the symmetric fission products increase with an increase of the neutron energy. This is due to the effect of the excitation energy, which will be discussed later. In contrast, Fig. 3 shows that for both the ^{232}Th(n, f) and ^{238}U(n, f), reactions, the yields of fission products for $A = 133$–134, 138–140, and 143–144, and their complementary products are higher than that of the other fission products. The asymmetric mass yield distribution with a triple-humped in the ^{232}Th(n, f) reaction and double-humped in the ^{238}U(n, f) reaction is due to the different type of potential energy surface between the two fissioning systems [63,64]. The fission products for $A = 133$–134, 138–140, and 143–144 have the most probable proton numbers of 52, 54, and 56, respectively. Thus, the oscillation of the fission yields in the interval of five mass units near the mass region of 133–144 and their complementary is due to the even–odd effect [16]. In addition, the higher yields of fission products for $A = 134$–134 and 143–144 are also due to the presence of spherical $82n$ and deformed $86-88n$ shells [13,14] based on the standard I and standard II asymmetric modes of fission [12]. As mentioned by Bross *et al.* [12], in standard I asymmetry, the fissioning system is characterized by spherical heavy fragment with mass numbers 133–134 due to the spherical $82n$ shell and a deformed complementary light mass fragment. Based on standard II asymmetry, the fissioning system is characterized by a deformed heavy-mass fragment near the mass numbers of 143–144 due to a deformed $86-88n$ shell and the slightly deformed light mass fragment. This is supported from the theoretical calculation of Scamps and Simenel [14], who have shown that the higher yields of fission products for $A = 134$–134 and 143–144

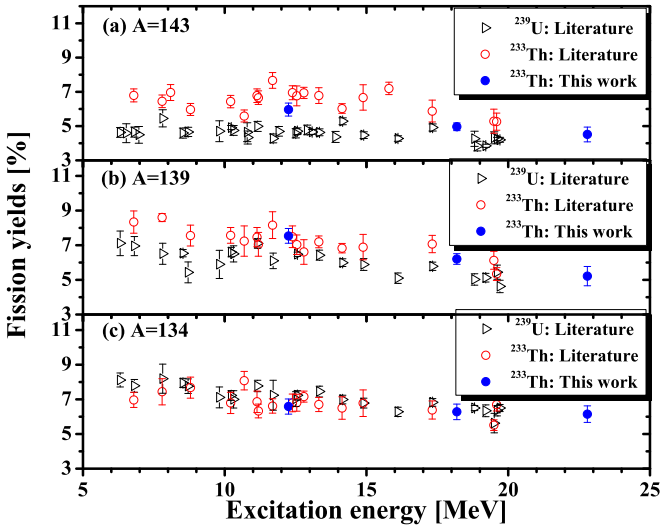

FIG. 4. Yield of fission products (%) as a function of excitation energy of compound nucleus for (a) $A = 143$, (b) $A = 139$, and (c) $A = 134$ for the ^{232}Th(n, f) and the ^{238}U(n, f) reactions.

corresponding to the $Z = 52$ and $Z = 56$ are due to the presence of the extra stability provided by octuple (pear-shaped) deformations in their fragments stage. According to them, the heavy fission fragments, which predominantly produced with 52 to 56 protons, are associated with substantial octuple deformation acquired on the way to fission. This has been proved by them [14] by using a quantum many-body model of superfluid fission dynamics [65]. They have also shown that the spherical doubly magic nuclei (e.g., $Z = 50$ and $N = 82$, i.e., ^{132}Sn) are very resistant to octuple deformation, which hinders their production as fission fragments.

From Fig. 3, it can be also seen that in the ^{232}Th(n, f) reaction, the fission yields for $A = 133$–134 and 143–144 are lower than for $A = 138$–140, whereas in the ^{238}U(n, f) reaction it is higher for $A = 133$–134 than for $A = 138$–140 and 143–144. This difference is clearly observed in Fig. 4, in which the yields of the fission products for $A = 133$, 139, and 143 from the present work and the literature data for the ^{232}Th(n, f) [19–43] and ^{238}U(n, f) reactions based on Refs. [54–56] and their back-references are plotted as a function of excitation energy. It is evident from Fig. 4 that for all excitation energies, the yields of the fission products for $A = 134$ and its complementary products are comparable for the ^{232}Th(n, f) and ^{238}U(n, f) reactions due to the presence of a strong spherical 82n shell. In contrast, the yields of fission products are marginally higher for $A = 139$ and significantly higher for $A = 143$ in the ^{232}Th(n, f) reaction compared to the ^{238}U(n, f) reaction. This difference cannot be explained using only the standard I and II asymmetry modes of fission [12] unless the shell combinations of the complementary fragments are considered. From the static scission model of Wilkins *et al.* [13] and its improved version by Andreev *et al.* [66], it is clear that a spherical shell of fission products exist for $Z = 28$, 50 and for $N = 50$, 82. Moreover, there also exists a deformed proton shell for $Z = 38$, 44, 56, and 66 as well as a deformed neutron shell for $N = 62$–66 and 86–88. Similarly, using a quantum many-body model of superfluid fission dynamics [63] with the incorporation of octuple deformation, Scamps and Simenel [14] show the spherical shell for $Z = 50$ and $N = 82$ as well as deformed shell for $Z = 52$, 56 and for $N = 84$, 88. In both the ^{232}Th(n, f) and ^{238}U(n, f) reactions, the fragments for $A = 133$–134 correspond to $Z = 52$ and, thus, have a spherical 82n shell if one neutron emission is considered. In the ^{232}Th(n, f) reaction, the complementary fragments for $A = 133$–134 have a deformed 38p shell. Similarly, in the ^{238}U(n, f) reaction, the light complementary fragments for $A = 133$–134 have a deformed 64n shell. Thus, the fission yields for $A = 133$–134 and their complementary are comparable in both the ^{232}Th(n, f) and ^{238}U(n, f) reactions. The fragment for $A = 143$–144 corresponds to $Z = 56$ and thus, has a deformed 86–88n shell if two neutrons emission are considered. The complementary fragments for $A = 143$–144 approach the spherical 50n shell in the ^{232}Th(n, f) reaction but not in the ^{238}U(n, f) reaction. Thus, the fission yields for $A = 143$–144 and their complementary are higher in the ^{232}Th(n, f) reaction than in the ^{238}U(n, f) reaction. In fact, the complementary fragments for $A = 143$–144 have an exact spherical 50n shell in the ^{229}Th(n, f) reaction [67,68]. Thus, the deformed 86–88n and spherical 50n shells combination cause the highest yields of 10–11% for $A = 144$ and its complementary $A = 84$ in the ^{229}Th(n, f) reaction [67,68], which support aforementioned observations. The fission yield fragments corresponding to $A = 138$–140 vary based on even–odd effect apart from a shell effect if it exists, which has been previously indicated. It is well-known that the even–odd factor decreases with an increase of the fissility parameter [15,16] and the excitation energy [69,70] of the fissioning systems. Thus, the marginal difference of the fission yields for $A = 138$–140 and their complementary products in both the ^{232}Th(n, f) and ^{238}U(n, f) reactions vanishes at higher excitation energies. The big difference of fission yields for $A = 143$–144 and their complementary products also vanishes at a higher excitation energy for the ^{232}Th(n, f) and ^{238}U(n, f) reaction, which may be due to the decrease of the even–odd effect with excitation energy. However, in both the ^{232}Th(n, f) and ^{238}U(n, f) reaction, the higher yields of fission products for $A = 133$–134, 138–140, and 143–144, and their complementary still persist at higher excitation energies, which can only be due to shell effects [13,14]. This observation indicates that although the even–odd effect decreases with an increase of the excitation energy but the shell effect still persists.

The variation of yields for $A = 133$–134, 139–140, and 143–144 in the ^{232}Th(n, f) and ^{238}U(n, f) reactions causes variation of the average heavy mass ($\langle A_H \rangle$) and accordingly, the average light mass ($\langle A_L \rangle$). The values of $\langle A_L \rangle$ and $\langle A_H \rangle$ in the ^{232}Th(n, f) reaction for average neutron energies of 7.46 MeV were calculated from the mass-chain yields (Y_A) of the fission products within the mass ranges of 80–105 and 125–150 using Eq. (9) given below. Similarly, for the average neutron energies of 13.4 and 18.0 MeV, the values of $\langle A_L \rangle$ were calculated from the mass-chain yields within the mass range of 80–105, whereas the values of $\langle A_H \rangle$ were calculated within the mass range of 124–149. This was done to maintain complementarity by assuming approximately three neutron emissions for the average neutron energy of 7.46 MeV and approximately four neutron emissions for the average neutron

TABLE II. Average light mass ($\langle A_L \rangle$), heavy mass ($\langle A_H \rangle$), and average neutron numbers ($\langle \upsilon \rangle_{\rm exp}$) for the neutron-induced fission of ^{232}Th.

Neutron energy (E_n) (MeV)	Excitation energy (E^*) (MeV)	$\langle A_L \rangle$	$\langle A_H \rangle$	$\langle \upsilon \rangle_{\rm exp}$	Ref.
2.0	6.79	90.9	139.8	2.3	[36]
3.0	7.79	91.2	139.4	2.4	[36]
4.0	8.79	91.3	139.1	2.6	[36]
5.42	10.21	91.7	138.6	2.7	[43]
5.9	10.69	91.9	138.4	2.7	[36]
6.35	11.14	91.6	138.4	2.9	[42]
6.4	11.19	91.1	138.9	3.0	[36]
6.9	11.51	90.5	139.1	3.4	[36]
7.46	12.25	90.9	138.9	3.2	[A]
7.6	12.39	90.8	138.9	3.3	[36]
7.75	12.54	91.4	138.4	3.2	[43]
8.0	12.79	90.9	138.8	3.3	[36]
8.53	13.32	91.3	138.4	3.4	[42]
9.35	14.14	91.4	138.1	3.5	[43]
10.09	14.88	91.6	138.1	3.5	[42]
12.53	17.32	91.6	137.9	3.5	[43]
13.4	18.19	91.5	137.9	3.7	[A]
14.7	19.49	91.5	137.7	3.8	[A,40]
14.8	19.59	93.3	135.8	3.9	[36,21]
18.0	22.79	91.6	137.3	4.1	[A]

energies of 13.4 and 18.0 MeV:

$$\langle A_L \rangle = \sum (Y_A A_L) \Big/ \sum Y_A, \qquad \langle A_H \rangle = \sum (Y_A A_H) \Big/ \sum Y_A. \tag{9}$$

From the $\langle A_L \rangle$, $\langle A_H \rangle$, and the compound nucleus mass ($A_C = 233$), the exact experimental average number of neutrons ($\langle \upsilon \rangle_{\rm exp}$) was calculated using the following relation:

$$\upsilon_{\rm exp} = A_C - (\langle A_L \rangle + \langle A_H \rangle). \tag{10}$$

The $\langle A_L \rangle$, $\langle A_H \rangle$, and $\langle \upsilon \rangle_{\rm exp}$ values in the ^{232}Th(n, f) reaction at the neutron energy of 14.7 MeV was also obtained from the literature data [40] using the same approach followed in the present work. This was done because at the neutron energy of 14.8 MeV, the $\langle A_L \rangle$ and $\langle A_H \rangle$ values given in Ref. [36] are based on the limited literature data [21]. Thus the $\langle A_L \rangle$, $\langle A_H \rangle$, and $\langle \upsilon \rangle_{\rm exp}$ values at 14.7 MeV, calculated from the data of Ref. [40] fits very well with the trend of the present work and other literature data [36,42,43]. The $\langle A_L \rangle$, $\langle A_H \rangle$, and $\langle \upsilon \rangle_{\rm exp}$ values as obtained from the preceding relations in the ^{232}Th(n, f) reaction along with their corresponding average excitation energy ($\langle E^* \rangle$) are given in Table II in addition to the literature data [36,42,43]. The $\langle A_L \rangle$ and $\langle A_H \rangle$ values for the ^{232}Th(n, f) reaction from Table II as well as for the ^{238}U(n, f) reaction from Refs. [54–56], along with the other literature data from their back-references as a function of excitation energy, are plotted in Fig. 5. The $\langle \upsilon \rangle_{\rm exp}$ values are plotted in Fig. 6.

Figure 5 shows that for all the excitation energy, the $\langle A_L \rangle$ values are significantly lower and the $\langle A_H \rangle$ values are higher

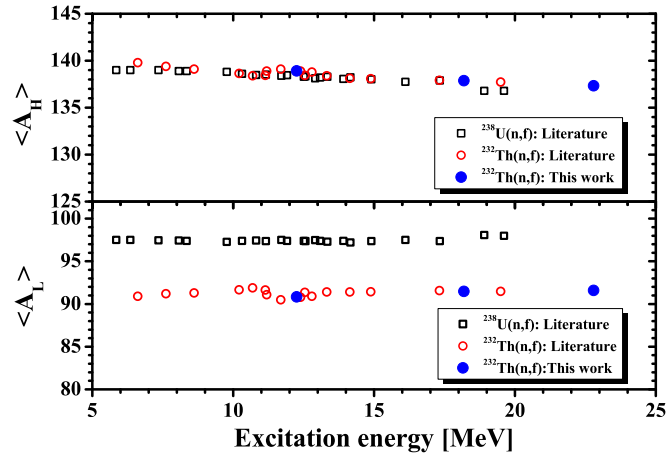

FIG. 5. The average values of heavy mass ($\langle A_H \rangle$) and the average values of light mass ($\langle A_L \rangle$) as a function of excitation energy of compound nucleus for the ^{232}Th(n, f) and the ^{238}U(n, f) reactions.

in the ^{232}Th(n, f) reaction than in the ^{238}U(n, f) reaction. The higher $\langle A_H \rangle$ values in the ^{232}Th(n, f) reaction are most probably due to the favorable standard II asymmetric mode compared to the standard I asymmetric mode of fission in the ^{232}Th(n, f) reaction. However, the $\langle A_L \rangle$ values in the ^{232}Th(n, f) reaction is significantly lower than that of the ^{238}U(n, f) reaction, which is due to mass conservation based on the standard I and II asymmetric modes of fission. It can also be seen from Fig. 5 that for both the ^{232}Th(n, f) and ^{238}U(n, f) reactions, the $\langle A_L \rangle$ values remain almost constant or increase slightly with the excitation energy, whereas the $\langle A_H \rangle$ values decrease with excitation energy. This is most probably due to the probability of more neutron emission from the heavy fragments [36]. In addition, Fig. 5 shows that the increasing trend of $\langle A_L \rangle$, as well as the decreasing trend of $\langle A_H \rangle$ with excitation energy is not smooth in the ^{232}Th(n, f) reaction compared to the ^{238}U(n, f) reaction. In the excitation energy range of 11–13 MeV, the increasing trend of $\langle A_L \rangle$ and the decreasing trend of $\langle A_H \rangle$ with excitation energy is very

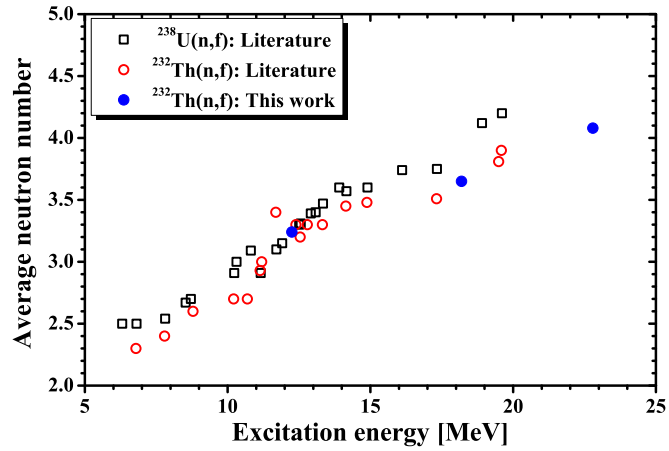

FIG. 6. The average neutron number ($\langle \upsilon \rangle_{\rm exp}$) as a function of excitation energy of compound nucleus for the ^{232}Th(n, f) and the ^{238}U(n, f) reactions.

distinct. This is due to the second chance fission around the excitation energies of 11–13 MeV in the ^{232}Th(n, f) reaction as explained in Ref. [36]. The role of excitation energy can be clearly observed in Fig. 6. It can be seen from Fig. 6 that the $\langle v \rangle_{\rm exp}$ value in both the ^{232}Th(n, f) and ^{238}U(n, f) reactions increases with excitation energy. Similar increase trend of $\langle v \rangle_{\rm exp}$ values in both the ^{232}Th(n, f) and ^{238}U(n, f) reactions is also observed from the experimental data by Manero and Konshin [71]. Further, Fig. 6 shows that except near the excitation energy values in the range of 11–13 MeV, the $\langle v \rangle_{\rm exp}$ value in the ^{232}Th(n, f) reaction is lower than that of the ^{238}U(n, f) reaction. The $\langle v \rangle_{\rm exp}$ value measured by Manero and Konshin [71] at all the excitation energies is also systematically lower in the ^{232}Th(n, f) reaction than in the ^{238}U(n, f) reaction. This is due to the lower fissility parameter for the fissioning system ^{233}Th* compared to ^{238}U. However, in the ^{232}Th(n, f) reaction, there is a remarkable difference between the experimental data of Fig. 6 and the measured data by Manero and Konshin [71] around the excitation energy of 11–13 MeV. Figure 6 shows that at an excitation energy of approximately 11–13 MeV, the $\langle v \rangle_{\rm exp}$ value in the ^{232}Th(n, f) reaction is slightly higher or comparable than in the ^{238}U(n, f) reaction, which is not the case in the measured data by Manero and Konshin [71]. So the abrupt higher $\langle v \rangle_{\rm exp}$ value in the ^{232}Th(n, f) reaction around the excitation energies of 11–13 MeV shown in Fig. 6 may be due to the indirect results obtained from the abrupt change of average light mass and heavy mass, which occur from the second chance fission.

As previously indicated, the two fissioning systems ^{233}Th* and ^{238}U have different potential energy surfaces [63,64]. Thus, the mass yield distribution in the ^{232}Th(n, f) reaction is asymmetric and triple-humped, whereas for the ^{238}U(n, f) reaction, it is asymmetric with a double hump, which was shown in Fig. 2. It can also be seen from Fig. 2 that in both the ^{232}Th(n, f) and ^{238}U(n, f) reactions, the yields of the symmetric fission products increase with neutron energy, which is the result of the effect of the excitation energy. In order to examine this aspect, the yields of symmetric products, high yield asymmetric products, and the peak-to-valley (P/V) ratios from the present work and literature data [19–43] for the ^{232}Th(n, f) reaction are shown in Table III. The yields of asymmetric and symmetric fission products from Table III for the ^{232}Th(n, f) reaction as well as for the ^{238}U(n, f) reaction from Refs. [54–56] along with literature data from their back-references as a function of excitation energy are shown in Fig. 7, whereas the P/V ratios are plotted in Fig. 8. It can be seen from Fig. 7 that for both the ^{232}Th(n, f) and ^{238}U(n, f) reactions, the yields of the asymmetric products decrease slightly, whereas the yields of the symmetric products increase significantly with excitation energy. Accordingly, the peak-to-valley (P/V) ratio (Fig. 8) decreases sharply with excitation energy for both the ^{232}Th(n, f) and ^{238}U(n, f) reactions. It can also be seen in Fig. 7 that the yields of the symmetric products below the excitation energy of 7.5 MeV are lower for the ^{232}Th(n, f) reaction than for the ^{238}U(n, f) reaction. Above the excitation energy of 7.5 MeV, the yields of the symmetric products are higher for the ^{232}Th(n, f) reaction than for the ^{238}U(n, f) reaction and increases with an increase of the excitation energy. This observation indicates that the

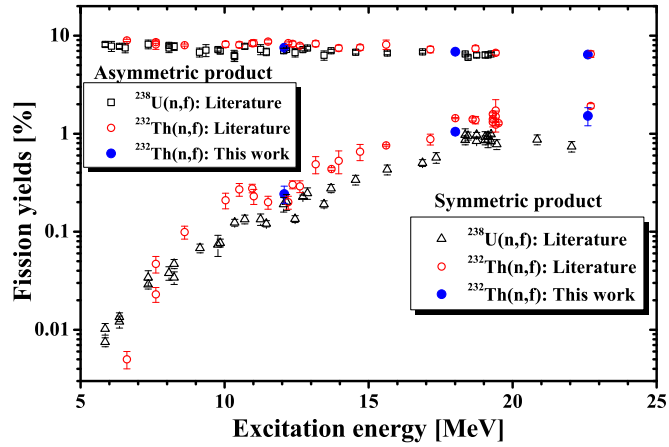

FIG. 7. The yield of the symmetric and asymmetric fission products (%) as a function of excitation energy of compound nucleus for the ^{232}Th(n, f) and the ^{238}U(n, f) reactions.

increasing trend of the yields for symmetric fission products and the decreasing trend of the P/V ratio with excitation energy is more pronounced for the ^{232}Th(n, f) reaction than for the ^{238}U(n, f) reaction. This is supported by the observation of Simutkin *et al.* [44,45] and Ryzhov *et al.* [46] based on the fission product yield data in the 10–60 MeV range for neutron-induced fission of ^{232}Th and ^{238}U measured using a physical technique. At the same neutron energy, symmetric fission is more enhanced in the ^{232}Th(n, f) reaction than in the ^{238}U(n, f) reaction.

Further, it can be seen from Fig. 7 that the yields of the symmetric products in the ^{232}Th(n, f) reaction increase sharply up to excitation energies of 11 MeV and then slightly decrease for values up to 13 MeV, and thereafter increase again. Thus, the P/V ratio in Fig. 8 for the ^{232}Th(n, f) reaction decreases sharply up to the excitation energy of 11 MeV, then slightly increases up to 13 MeV, followed by a decrease. The higher yield of symmetric products and lower P/V ratio in the ^{232}Th(n, f) reaction within the excitation energy of 11–13 MeV are due to the second chance

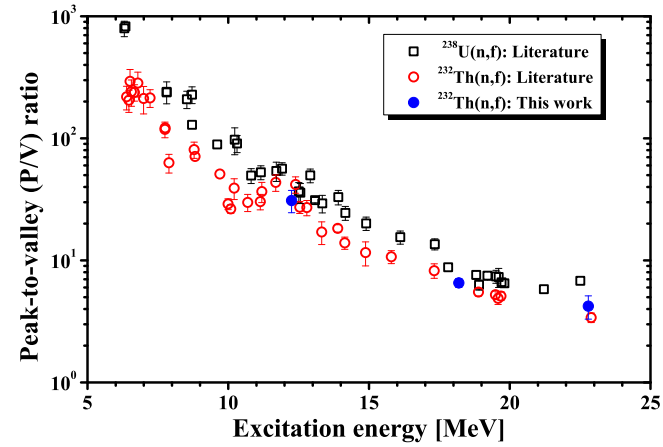

FIG. 8. The peak-to-valley (P/V) ratio as a function of excitation energy of compound nucleus for the ^{232}Th(n, f) and the ^{238}U(n, f) reactions.

TABLE III. Yield of asymmetric (Y_a) and symmetric (Y_s) products and the P/V ratio in the neutron-induced fission of ^{232}Th.

Neutron energy (E_n) (MeV)	Excitation energy (E^*) (MeV)	Y_a(%)	Y_s(%)	P/V	Ref.
1.60 ± 0.02	6.39	—	—	2 18.9 ± 47.7	[35]
1.68 ± 0.02	6.47	—	—	205.1 ± 42.1	[35]
1.72 ± 0.02	6.51	—	—	292.7 ± 73.2	[35]
1.77 ± 0.02	6.56	—	—	241.5 ± 58.8	[35]
1.88 ± 0.02	6.67	—	—	238.2 ± 36.5	[35]
2.00 ± 0.02	6.79	—	—	283.5 ± 64.9	[35]
2.00	6.79	8.950 ± 0.250	0.005 ± 0.001	—	[36]
2.20 ± 0.02	6.99	—	—	212.3 ± 53.9	[35]
2.43 ± 0.02	7.22	—	—	214.5 ± 35.6	[35]
2.96 ± 0.41	7.75	—	—	118.5 ± 17.5	[35]
2.97	7.76	—	—	122.0	[31]
3.00	7.79	8.600 ± 0.230	0.023 ± 0.004	—	[36]
3.00	7.79	7.890 ± 0.094	0.045 ± 0.009	—	[21]
3.10 ± 0.15	7.89	—	—	63.0 ± 11.0	[37]
4.00	8.79	8.010 ± 0.200	0.099 ± 0.015	80.9 ± 12.3	[36]
4.03 ± 0.02	8.82	—	—	71.0	[31]
4.20 ± 0.11	8.99	—	—	27.2 ± 3.1	[35]
4.81 ± 0.02	9.60	—	—	51.0	[31]
5.20 ± 0.25	9.99	—	—	29.0 ± 3.0	[37]
5.30 ± 0.11	10.09	—	—	26.4 ± 2.1	[35]
5.42	10.21	8.177 ± 0.574	0.209 ± 0.038	39.1 ± 7.6	[43]
5.90	10.69	8.080 ± 0.530	0.270 ± 0.040	29.9 ± 4.8	[36]
6.35	11.14	8.358 ± 0.551	0.277 ± 0.028	30.3 ± 4.4	[42]
6.40	11.19	8.410 ± 0.630	0.230 ± 0.040	36.6 ± 6.9	[36]
6.90	11.69	8.700 ± 0.340	0.200 ± 0.030	43.5 ± 6.7	[36]
7.46	12.25	7.540 ± 0.430	0.243 ± 0.048	31.0 ± 6.4	[A]
7.60	12.39	8.380 ± 0.230	0.200 ± 0.030	41.9 ± 6.4	[36]
7.75	12.54	8.240 ± 0.524	0.302 ± 0.028	27.3 ± 3.1	[43]
8.00	12.89	7.870 ± 0.350	0.290 ± 0.030	27.1 ± 3.9	[36]
8.53	13.32	8.299 ± 0.579	0.487 ± 0.097	17.1 ± 3.6	[42]
9.10 ± 0.30	13.89	(8.000 ± 0.500)	0.436 ± 0.014	18.3 ± 1.3	[22]
10.09	14.88	7.579 ± 0.491	0.655 ± 0.123	11.6 ± 2.6	[42]
11.00	15.79	8.100 ± 0.900	0.760 ± 0.015	10.7 ± 1.3	[20]
12.53	17.32	7.237 ± 0.545	0.879 ± 0.112	8.24 ± 1.12	[43]
13.4	18.19	6.864 ± 0.345	1.033 ± 0.156	6.64 ± 1.06	[A]
13.40 ± 0.17	18.19	(7.500 ± 0.500)	1.440 ± 0.020	5.21 ± 0.35	[22]
14.10 ± 0.16	18.89	(7.500 ± 0.500)	1.340 ± 0.020	5.60 ± 0.38	[22]
14.70 ± 0.30	19.49	(7.500 ± 0.500)	1.580 ± 0.050	4.75 ± 0.51	[40]
14.70 ± 0.30	19.49	—	1.400 ± 0.050	5.36 ± 0.41	[40]
14.70 ± 0.30	19.49	—	1.310 ± 0.140	5.73 ± 0.72	[28]
14.70 ± 0.30	19.49	—	1.380 ± 0.120	5.43 ± 0.59	[38]
14.80 ± 0.80	19.59	6.690 ± 0.325	1.720 ± 0.500	3.89 ± 1.15	[21]
14.80 ± 0.80	19.59	—	1.500 ± 0.200	4.46 ± 0.65	[24]
14.80 ± 0.80	19.59	—	1.240 ± 0.200	5.40 ± 0.92	[23]
14.90 ± 0.25	19.69	(6.500 ± 0.500)	1.280 ± 0.040	5.10 ± 0.42	[22]
18.0	22.79	6.406 ± 0.324	1.522 ± 0.318	4.21 ± 0.91	[A]
18.10 ± 0.25	22.89	(6.500 ± 0.500	1.920 ± 0.100	3.40 ± 0.31	[22]

fission as mentioned in Ref. [36]. A similar effect within the excitation energy range of 11–13 MeV was also observed in the proton-induced fission of ^{232}Th [72], which supports our observation. For the ^{238}U(n, f) reaction, the increase of the yield of the symmetric products and the decrease of the P/V ratio is nearly smooth or varies slightly within the excitation energy range of 11–13 MeV. The different behavior of the ^{232}Th(n, f) reaction compared to the ^{238}U(n, f) reaction in the excitation energy range of 11–13 MeV is due to the different extent of second chance fission in the former than in the latter. It can also be seen from Fig. 8 that for all the excitation energies, the P/V ratio in the ^{232}Th(n, f) reaction is lower than that in the ^{238}U(n, f) reaction. This is due to the different type of potential energy surfaces in ^{233}Th* compared to ^{239}U* [63,64] as previously indicated, apart from the role of the excitation energy.

V. CONCLUSIONS

(i) The cumulative yields of 48 fission products in the ^{232}Th(n, f) reaction with average neutron energies of 7.46, 13.4, and 18.0 MeV were measured using an off-line γ-ray spectrometric technique. From the cumulative yields of product, mass yields for 42 isobaric chains were obtained by exploiting charge distribution correction. It was found that the mass-yield distributions in the ^{232}Th(n, f) reaction is triple-humped unlike in the ^{238}U(n, f) reaction, which is double-humped. This is due to the different type of potential energy surfaces in ^{232}Th* compared to ^{239}U*.

(ii) In both the ^{232}Th(n, f) and ^{238}U(n, f) reactions, the yields of fission products for $A = 133$–134, $A = 138$–140, and $A = 143$–144, and their complementary products are higher than those of other fission products. This is due to shell closure proximity based on the static scission point model and the superfluid dynamic model with octuple deformations apart from the role of the even–odd effect. It was found that the ^{232}Th(n, f) reaction is favorable due to the standard II asymmetric mode of fission whereas, the ^{238}U(n, f) reaction is favorable due to the standard I asymmetric mode of fission.

(iii) In both the ^{232}Th(n, f) and ^{238}U(n, f) reactions, the $\langle v\rangle$ and $\langle A_L\rangle$ values increase and the $\langle A_H\rangle$ values decrease with excitation energy. However, within the excitation energy range of 11–13 MeV, the increasing trend of $\langle v\rangle_{\rm exp}$ and $\langle A_L\rangle$ and the decreasing trend of $\langle A_H\rangle$ with excitation energy is distinct for the ^{232}Th(n, f) reaction, which is due to the second chance fission.

(iv) The yield of asymmetric products for both the ^{232}Th(n, f) and ^{238}U(n, f) reactions decreased marginally, whereas for symmetric products, there was a sharp increase with excitation energy. In the ^{232}Th(n, f) reaction, the yield of symmetric products increases sharply up to the excitation energy of 11 MeV, then decreased up to 13 MeV. This was followed by an increase with excitation energy beyond 13 MeV. The decrease trend of yield for symmetric fission products within the excitation energy of 11–13 MeV is due to the second chance fission. In the ^{238}U(n, f) reaction, the increase of the yield of symmetric product fission did not vary significantly and was lower than that of the ^{232}Th(n, f) reaction above an excitation energy of 7.5 MeV.

(v) In both the ^{232}Th(n, f) and ^{238}U(n, f) reactions, the P/V ratios decrease with excitation energy. However, for all excitation energies, the P/V ratio in the ^{232}Th(n, f) reaction is lower than that of the ^{238}U(n, f) reaction, which is due to the effect of different type of potential energy surfaces between two the fissioning systems apart from the role of the excitation energy.

ACKNOWLEDGMENTS

The authors express their sincere thanks to the staff of the MC-50 Cyclotron in KIRAMS for their excellent operation and their support during the experiments. This research was partly supported by the National Research Foundation of Korea through a grant provided by the Ministry of Science, ICT, and Future Planning (Grants No. NRF-2017R1D1A1B03030484, No. NRF-2018M7A1A1072274, and No. NRF-2018R1A6A1A06024970).

[1] K. Oyamatsu, H. Takeuchi, M. Sagisaka, and J. Katakura, J. Nucl. Sci. Techol. **38**, 477 (2001).
[2] T. R. Allen and D. C. Crawford, Sci. Technol. Nucl. Install. **2007**, 97486 (2007).
[3] A. Nuttin, D. Heuer, A. Billebaud, R. Brissot, C. Le Brun, E. Liatard, J. M. Loiseaux, L. Mathieu, O. Meplan, E. Merle-Lucotte, H. Nifenecker, F. Perdu, and S. David, Progr. Nucl. Energy **46**, 77 (2005).
[4] Thorium fuel utilization: Options and Trends, IAEA, Vienna, IAEA Report IAEA-TECDOC-1319 (2002).
[5] L. Mathieu *et al.*, Proportion for a very simple thorium molten salt reactor, in *Proceedings of the Global International Conference* (Tsukuba, Japan, 2005).
[6] R. K. Sinha and A. Kakodkar, Nucl. Eng. Des. **236**, 683 (2006).
[7] F. Carminati, R. Klapisch, J. P. Revol, Ch. Roche, J. A. Rubia, and C. Rubia, An energy amplifier for cleaner and inexhaustible nuclear energy production Driven by particle beam accelerator, CERN Report CERN/AT/93-49 (ET) (1993).
[8] C. Rubia, J. A. Rubio, S. Buono, F. Carminati, N. Fietier, J. Galvez, C. Geles, Y. Kadi, R. Klapisch, P. Mandrilion, J. P. Revol, and Ch. Roche, CERN Report CERN/LHC/97-01 (EET) (1997).
[9] C. D. Bowman, Annu. Rev. Nucl. Part. Sci. **48**, 505 (1998).
[10] C. Wagemans, *The Nuclear Fission Process* (CRC, London, 1990).
[11] R. Vandenbosch and J. R. Huizenga, *Nuclear Fission* (Academic, New York, 1973).
[12] U. Brossa, S. Grossmann, and A. Muller, Phys. Rep. **197**, 167 (1990).
[13] B. D. Wilkins, E. P. Steinberg, and R. R. Chasman, Phys. Rev. C **14**, 1832 (1976).
[14] G. Scamps and C. Simenel, Nature **564**, 382 (2018).
[15] H. Naik, S. P. Dange, R. J. Singh, and S. B. Manohar, Nucl. Phys. A **612**, 143 (1997).
[16] H. Naik, R. J. singh, and R. H. Iyer, Eur. Phys. J. A **16**, 495 (2003).
[17] R. H. Iyer, C. K. Mathews, N. Ravindran, K. Rengan, D. V. Singh, M. V. Ramaniah, and H. D. Sharma, J. Inorg. Nucl. Chem. **25**, 465 (1963).
[18] H. N. Erten, A. Grutter, E. Rossler, and H. R. von Gunten, Nucl. Sci. Eng. **79**, 167 (1981).
[19] A. Turkevich and J. B. Nidday, Phys. Rev. **84**, 52 (1951).
[20] A. Turkevisch, J. B. Nidday, and A. Tompkins, Phys. Rev. **89**, 552 (1953).
[21] K. M. Broom, Phys. Rev. **133**, B874 (1964).
[22] G. P. Ford and R. B. Leachman, Phys. Rev. **137**, B826 (1965).

[23] R. Ganapathy and P. K. Kuroda, J. Inorg. Nucl. Chem. **28**, 2071 (1966).
[24] Tin Mo and M. N. Rao, J. Inorg. Nucl. Chem. **30**, 345 (1968).
[25] M. Thin, M. N. Rao, and P. K. Kurdo, J. Inorg. Nucl. Chem. **30**, 1145 (1968).
[26] A. I. Sagachev, V. G. Vorobeieva, B. D. Kuzminov, V. B. Mikhaylov, and Z. Tarsko, Sov. J. Nucl. Phys. **7**, 475 (1968).
[27] S. J. Lyle and J. Sellears, Radiochim. Acta **12**, 43 (1969).
[28] L. H. Gevaert, R. E. Jervis, and H. D. Sharma, Can. J. Chem. **48**, 641 (1970).
[29] J. Blachot, L. C. Carraz, P. Cavallini, E. Monnand, and F. Schusslor, J. Radioanal. Nucl. Chem. **7**, 309 (1971).
[30] D. L. Swindle, D. T. Moore, J. N. Beck, and P. K. Kuroda, J. Inorg. Nucl. Chem. **33**, 3643 (1971).
[31] W. Holubarsch, L. Pfeiffer, and F. Gonnenwein, Nucl. Phys. A **171**, 631 (1971).
[32] S. A. Rao, Phys. Rev. C **5**, 171 (1972).
[33] J. P. Bocquet, R. Brissot, J. Crancon, and A. Moussa, Nucl. Phys. A **189**, 556 (1972).
[34] S. M. Dubroviva, V. I. Nogorodtseva, L. N. Morozov, V. A. Pchevin, L. V. Chistyakov, V. A. Schigin, and V. M. Shubko, Yad. Fiz. **17**, 1470 (1973).
[35] J. Trochon, H. A. Yehia, F. Brisard, and Y. Pranal, Nucl. Phys. A **318**, 63 (1979).
[36] L. E. Glendenin, J. E. Gindler, I. Ahmad, D. J. Henderson, and J. W. Meadows, Phys. Rev. C **22**, 152 (1980).
[37] S. T. Lam, L. L. Yu, H. W. Fielding, W. K. Dawson, and G. C. Neilson, Phys. Rev. C **28**. 1212 (1983).
[38] A. E. Richoortson, H. L. Wright, J. L. Meason, and J. R. Smith, Nucl. Sci. Eng. **94**, 413 (1986).
[39] Li. Wenxin, S. Tongyu, S. Xiuhua, Fu Ming, and D. Tianrong, High Energy Phys. and Nucl. Phys. **3**, 376 (1987) (Chinese).
[40] S. Tongyu, Li Wenxin, D. Tianrong, and Fu Ming, High Energy Phys. and Nucl. Phys. **2**, 221 (1988) (Chinese).
[41] P. M. Prajapati, H. Naik, S. Mukherjee, S. V. Suryanarayana, B. S. Shivashankar, R. Crasta, V. K. Mulik, K. C. Jagadeesan, S. V. Thakre, and A. Goswami, Nucl. Sci. Eng. **176**, 106 (2014).
[42] H. Naik, Rita Crasta, S. V. Suryanarayana, P. M. Prajapati, V. K. Mulik, B. S. Shivasankar, K. C. Jagadeesan, S. V. Thakare, S. C. Sharma, and A. Goswami, Eur. Phys. J. A. **50**, 144 (2014).
[43] H. Naik, Sadhana Mukherji, S. V. Suryanarayana, K. C. Jagadeesan, S. V. Thakare, and S. C. Sharma, Nucl. Phys. A **952**, 100 (2016).
[44] V. D. Simutkin, I. V. Ryzhov, G. A. Tutin, L. A. Vaishnene, J. Blomgren, S. Pomp, M. Österlund, P. Andersson, R. Bevilacqua, J. P. Menlders, and R. Prieels, in *4th International Workshop on Nuclear Fission and Fission-Product Spectroscopy*, edited by A. Chatillon, H. Faust, G. Fioni, D. Goutte, and H. Goutte, AIP Conf. Proc. No. 1175 (AIP, New York, 2009), p. 393.
[45] V. D. Simutkin, S. Pomp, J. Blomgren, M. Österlund, R. Bevilacqua, P. Andersson, I. V. Ryzhov, G. A. Tutin, S. G. Yavshits, L. A. Vaishnene, M. S. Onegin, J. P. Meulders, and R. Prieels, Nucl. Data Sheets **119**, 331 (2014).
[46] I. V. Ryzhov, S. G. Yavshits, G. A. Tutin, N. V. Kovalev, A. V. Saulski, N. A. Kudryashev, M. S. Onegin, L. A. Vaishnene, Yu. A. Gavrikov, O. T. Grudzevich, V. D. Simutkin, S. Pomp, J. Blomgren, M. Österlund, P. Andersson, R. Bevilacqua, J. P. Meulders, and R. Prieels, Phys. Rev. C **83**, 054603 (2011).
[47] A. C. Wahl, At. Data Nucl. Data Tables **39**, 1 (1988).
[48] H. Umezawa, S. Baba, and H. Baba, Nucl. Phys. A **160**, 65 (1971).
[49] IAEA-EXFOR Database, Experimental nuclear reaction data, available at http://www-nds.iaea.org/exfor/.
[50] N. L. Borisova, S. M. Dubrovina, V. I. Novgorodtseva, V. A. Pchelin, V. A. Shigin, and V. M. Shubko, Yad. Fiz. **6**, 454 (1967) [Sov. J. Nucl. Phys. **6**, 331 (1968)].
[51] M. Rajagopalan, H. S. Pruys, A. Grutter, E. A. Hermes, and H. R. von Gunten, J. Inorg. Nucl. Chem. **38**, 351 (1976).
[52] T. C. Chapman, G. A. Anzelon, G. C. Spitale, and D. R. Nethaway, Phys. Rev. C **17**, 1089 (1978).
[53] S. Nagy, K. F. Flynn, J. E. Gindler, J. W. Meadows, and L. E. Glendenin, Phys. Rev. C **17**, 163 (1978).
[54] H. Naik, V. K. Mulik, P. M. Prajapati, B. S. Shivasankar, S. V. Suryanarayana, K. C. Jagadeesan, S. V. Thakare, S. C. Sharma, and A. Goswami, Nucl. Phys. A **913**, 185 (2013).
[55] S. Mukerji, H. Naik, S. V. Suryanarayana, B. S. Shivashankar, V. K. Mulik, A. Goswami, and P. D. Krishnani, J. Korean Phys. Soc. **65**, 18 (2014).
[56] H. Naik, Sadhana Mukerji, Rita Crasta, S. V. Suryanarayana, S. C. Sharma, and A. Goswami, Nucl. Phys. A **941**, 16 (2015).
[57] C. M. Zöeller, A. Gavron, J. P. Lestone, M. Mutterer, J. P. Theobald, A. S. Iljinov, and M. V. Mebel, in *Proceedings of the Seminar on Fission Pont d'Oye III*, edited by C. Wagemans, and P. D'hondt (Haby-la-Neuve, Belgium, 1995).
[58] J. S. Hendricks, W. M. Gregg, L. F. Michael, R. J. Michael, C. J. Russell, W. D. Joe, P. F. Joshua, B. P. Denise, S. W. Laurie, and W. M. William, MCNPX 2.6.0 Extensions, LANL Report LA-UR-08-2216, Los Alamos (2008), available at http://mcnpx.lanl.gov/.
[59] J. K. Tuli, Nuclear Wallet Cards (2011), available at http://www.nndc.bnl.gov.
[60] NuDat 2.6, National Nuclear Data Center, Brookhaven National Laboratory, updated 2011, available at http://www.nndc.bnl.gov/.
[61] S. Y. F. Chu, L. P. Ekstrom, and R. B. Firestone, in *WWW Table of Radioactive Isotopes* (The Lund LBNL, Nuclear Data Search, Version 2.0, February 1999), available at http://nucleardata.nuclear.lu.se/toi/.
[62] N. Sugarman and A. Turkevich, in *Radiochemical Studies: The Fission Product*, edited by C. D. Coryell and N. Sugarman, Vol. 3 (McGraw-Hill, New York, 1951), p. 1396.
[63] P. Moller, Nucl. Phys. A **192**, 529 (1972).
[64] P. Moller, D. G. Madland, A. J. Sierk, and A. Iwamoto, Nature (London) **409**, 785 (2001).
[65] G. Scamps, C. Simenel, and D. Lacroix, Phys. Rev. C **92**, 011602(R) (2015).
[66] A. V. Andreev, G. G. Adamian, and N. V. Antonenko, Phys. Rev. C **86**, 044315 (2012).
[67] M. Haddad, J. Crancon, G. Lhospice, M. Asghar, and J. Blachot, Radiochim. Acta **42**, 165 (1987).
[68] C. Agarwal, A. Goswami, P. C. Kalsi, S. Singh, A. Mhatre, and A. Ramaswami, J. Radioanal. Nucl. Chem. **275**, 445 (2008).
[69] S. Amiel, H. Feldstein, and T. Izak-Biran, Phys. Rev. C **15**, 2119 (1977).
[70] G. Mariolopoulos, Ch. Hamelin, J. Blachot, J. P. Bocquet, R. Brissot, J. Crancon, H. Nifenecker, and Ch. Ristori, Nucl. Phys. A **361**, 213 (1981).
[71] F. Manero and A. V. Konshin, At. Energy Rev. **10**, 637 (1972).
[72] H. Kudo, H. Muramatsu, H. Nakahara, K. Miyano, and I. Kohno, Phys. Rev. C **25**, 3011 (1982).